

We are IntechOpen, the world's leading publisher of Open Access books Built by scientists, for scientists

6,900

Open access books available

185,000

International authors and editors

200M

Downloads

Our authors are among the

154

Countries delivered to

TOP 1%

most cited scientists

12.2%

Contributors from top 500 universities



WEB OF SCIENCE™

Selection of our books indexed in the Book Citation Index
in Web of Science™ Core Collection (BKCI)

Interested in publishing with us?
Contact book.department@intechopen.com

Numbers displayed above are based on latest data collected.
For more information visit www.intechopen.com



A CFD Porous Materials Model to Test Soil Enriched with Nanostructured Zeolite Using ANSYS-Fluent^(TM)

Diana Barraza-Jiménez, Sandra Iliana Torres-Herrera, Patricia Ponce Peña, Carlos Omar Ríos-Orozco, Adolfo Padilla Mendiola, Elva Marcela Coria Quiñones, Raúl Armando Olvera Corral, Sayda Dinorah Coria Quiñones and Manuel Alberto Flores-Hidalgo

Abstract

Soil health is a great concern worldwide due to the huge variety of pollutants and human activities that may cause damage. There are different ways to remediate and make a better use of soil and a choice may be using zeolite in activities like gardening, farming, environment amending, among others. In this work is proposed a model to simulate how mixing zeolite with soil may be beneficial in different ways, we are especially interested in interactions of mixed soil-zeolite with water. This model is based in different flow regimes where water interacts with two layers formed by nanostructured zeolite and soil in a vertical arrangement. The analysis is approached as a bi-layer porous material model resolved by using the mathematical model implemented in ANSYS-Fluent. Such model uses a multi-fluid granular model to describe the flow behavior of a fluid–solid mixture where all the available interphase exchange coefficient models are empirically based. Despite the great capabilities of numerical simulation tools, it is known that at present time, the literature lacks a generalized formulation specific to resolve this kind of phenomena where a porous media is analyzed. This model is developed to obtain a systematic methodology to test nanomaterials with porous features produced in our laboratory which is the next step for near future work within our research group.

Keywords: porous, CFD, ANSYS-Fluent®, soil, nanostructured zeolite

1. Introduction

A porous material is a complex structure consisting of a compact phase (usually solid) and some void space, which relates directly with the term porosity. The literature describes a porous medium as a region in space comprising of at least two homogeneous material constituents, presenting identifiable interfaces between them in a resolution level, with at least one of its constituents remaining fixed or

slightly deformable [1]. Among porous materials, soil and zeolite are interesting because they are perfectly aligned with the definition for porous materials.

The aim of this work is search for options to improve soil health since it is a great concern worldwide due to the huge variety of pollutants and anthropogenic activities that may cause damage. Zeolite is an option to amend soil in activities like gardening, farming, environment amending, among others, it is reported in the literature as a suitable material for sustainable chemistry. Mixing zeolite in soil may be beneficial in different ways, we are especially interested in interactions of mixed soil-zeolite with water. In this work, a model is developed to obtain a systematic methodology to test nanomaterials with porous features produced in our laboratory which is the next step for near future work within our research group. This model is based in different flow regimes where water interacts with two layers formed by nanostructured zeolite and soil in a vertical arrangement. The analysis is approached as a bi-layer porous material model resolved using the mathematical model implemented in ANSYS-Fluent.

2. Fundamental concepts

In this section a brief set of fundamental concepts are displayed to put the reader in context with the topics within this research work as described next.

2.1 Porous materials

The word *porous* describes a structure with a compact phase (usually solid) and some void (empty) space. Any solid material containing cavities, channels or interstices may be considered porous. Concepts like “pores”, “cavities”, among others, are features for a porous material and according to them, such material may be characterized. The reader is referred to the literature on porous materials for more information on the correct use of related terms [1–5]. Our recommended definition for the context of the present work is “*A porous medium is a region in space comprising of at least two homogeneous material constituents, presenting identifiable interfaces between them in a resolution level, with at least one of the constituents remaining fixed or slightly deformable*” [2]. Measurements are important to characterize porous materials, one may be interested in pore size range, performance at different levels of compression and/or temperature, performance when interacting with different liquids, repeatability, structures, corrugated pores, etc. [1] Even though, porous materials latest breakthrough was reported over a decade ago, there are still plenty of interesting applications that use this type of materials [4] and new techniques to prepare them. Also, over the last ten years or so, literature highlights include synthesis, applications, hierarchically structured porous materials [1–6], among others.

Porous materials are defined as elements/compounds that contain a porous structure consisting of interconnected pores on different length scales from micro- (<2 nm), meso- (2–50 nm) to macropores (>50 nm). Micro- and mesopores may provide size and shape selectivity for guest molecules, enhancing the host–guest interactions. Alternatively, macropores can considerably favor diffusion to and accessibility of active sites by guest molecules, which is particularly important for the diffusion of large molecules or in viscous systems. Emphasis in porous size is an important work trend among scientists and technologists due to the wide range of possibilities regarding applications of porous materials based in pore size. One of the more interesting porous materials is zeolites which are included within this study [5–7].

2.2 Zeolites

Zeolites were found in 1756 and since then their use has spread out in chemical industries for catalysis, adsorption, separation, and a great variety of other applications. 35,232 patents with the title including “zeolite*” are documented by Derwent Innovations Index as of January 2, 2020 and around 30,271 publications with “zeolite*” in their title are recorded by the Web of Science Core Collection in the same date. Although there is a lot of work and advancement in the science and technology related to zeolites, fundamental research on them and their applications have a great deal of relevancy [5].

Zeolites in its natural mineral presentation are found in several parts of the world but most zeolites used are produced by synthesis [8, 9]. Differences between natural and synthetic zeolites include: 1) Synthetics are obtained from chemicals and naturals are processed mines, 2) Synthetic zeolites silica to alumina ratio is 1 to 1 and natural clinoptilolite zeolites is 5 to 1 ratio, 3) clinoptilolite zeolite do not break down in mildly acid environment, synthetic zeolites do break. Natural zeolite structure has more acid resistant silica to keep its structure together [9].

Zeolite is a microporous (<2 nm) material comprising crystalline aluminosilicate with various structures [10, 11]. Over 200 types of zeolites have been reported [12] with pore diameters between 0.25 and 1 nm [13] and possess good selectivity properties [14–16]. In catalytic applications, zeolite framework structure is an assembly made of AlO_4 and SiO_4 tetrahedra able to provide Brønsted and Lewis acid sites inside the micropore [17–20]. For example, Brønsted acid sites in synthetic zeolites, such as zeolite Y and ZSM-5, are responsible for the catalytic cracking reaction in oil refinery [21].

Hierarchical porous zeolite addresses issues with porous size. Under its perspective, there are three types of porosity according to pore size, micropore (<2 nm), mesopore (2–50 nm), and macropore (>50 nm) [22]. Zeolites may be considered a family of crystalline aluminosilicates consisting of orderly distributed molecular sized nanopores. Their structure benefits adsorption of guest molecules with specific sizes and shapes or separation processes for liquid or gas mixtures as molecular sieves [23, 24]. In addition, zeolites with guest species, coupled with acid or metal sites, enables shape-selective catalysis [25–27]. Zeolites are considered the most important solid catalysts in petrochemical industries [28–31]. Zeolitic materials are also promising in a wide variety of applications, including renewable energy and environmental improvement [32].

Properties of zeolites are directly related with their nanoporous framework structures, so TO_4 tetrahedra (“T” denotes tetrahedrally coordinated Si, Al, P, etc.) is fundamental [33]. According to the literature [22], 235 types of zeolite frameworks have been discovered [12], however, there is still a high demand for improved zeolitic materials with new structures and superior functions. In addition, new technology trends are giving a new impulse to zeolite research, such is the case of nanotechnology where nanostructured zeolite or interactions of zeolite with nanostructured materials have captured the interest of researchers. Soil may be counted among the more interesting interactions with zeolite.

2.3 Soil

The Soil Science Society of America has published two definitions for soil. One is “*The unconsolidated mineral or organic material on the immediate surface of the earth that serves as a natural medium for the growth of land plants.*” The second definition may be more inclusive and says soil is “*The unconsolidated mineral or organic matter on the surface of the earth that has been subjected to and shows the effects of genetic and*

environmental factors of: climate (including water and temperature effects) and macro- and microorganisms, conditioned by relief, acting on parent material over a period of time” [34, 35].

A soil detailed definition depends upon physical, chemical, biological, and morphological properties, and characteristics. Their effect on soil management decisions is critical in any case the soil is to be used in either crop production, in an urban setting, or for roads, dams, waste disposal, and other uses [35].

Soil is a porous media at the land surface formed by weathering processes mediated by biological, geological, and hydrological phenomena. Soil is different than weathered rock because it shows a vertical stratification (the soil horizons) that has been produced by the influence of percolating water and living organisms. From a chemistry perspective, soils are open, multicomponent, biogeochemical systems containing solids, liquids, and gases. Open systems mean soils exchange matter and energy with the surrounding atmosphere, biosphere, and hydrosphere. Such exchange is highly variable, but it is the essential flux that cause the development of soil profiles and the patterns of soil quality [36].

Generally, soil is formed by fragmented and chemically weathered rock which includes sand, silt, and clay separates, and contains humus (partially decomposed organic matter). Soil diversity is huge, because of the different regional circumstances, it varies considerably. If properties of soil are known, it may be effectively managed and succeed at a specific use or purpose.

The major elements in soils exceed a concentration of $100 \text{ mg}\cdot\text{kg}^{-1}$, all others are known as trace elements. According to multiple reports, the major elements include O, Si, Al, Fe, C, K, Ca, Na, Mg, Ti, N, S, Ba, Mn, P, and perhaps Sr and Zr, in decreasing order of concentration. The major elements C, N, P, and S also are macronutrients, so they are critical to life cycles and may be absorbed by organisms in significant amounts [36].

2.4 Water and drought

Climate change is affecting the way we live without a doubt. For example, El Nino and La Nina are climate patterns in the Pacific Ocean that affect weather worldwide [10]. In Mexico, these and other climate related phenomena are responsible for intensified drought in a great part of the country. In the northern part of Mexico for this year (2021) the forecast indicates there will be 20–30% water availability for the different activities if compared to last year [11]. Porous materials may be a feasible option for gardens and crop soil to keep humidity for longer periods of time. Then, porous materials and specially zeolite, are interesting materials for studying their interaction with soil and water.

3. Methodology

In this work is used the code ANSYS-Fluent® [37, 38] and all CFD methodologies presented are embedded in this program. Like most CFD codes, ANSYS contains three main elements: (a) a preprocessor, (b) a solver, and (c) a postprocessor, the role of each one will be described briefly in the next sections.

ANSYS Fluent solves conservation equations for mass and momentum. For flows involving heat transfer or compressibility, an additional equation for energy conservation is solved. Additional transport equations are solved when the flow has other features such as transport species, chemical reactions, turbulence, etc. Since conservation equations are widely known, we will present only the simplified version and will focus in describing the porous media approach briefly.

The equation for conservation of mass, or continuity equation, can be written as follows:

$$\frac{\partial \rho}{\partial t} + \nabla \cdot (\rho \vec{v}) = S_m \quad (1)$$

Eq. (1) is the general form of the mass conservation equation and is valid for incompressible as well as compressible flows. The source S_m is the mass added to the continuous phase from the dispersed second phase (for example, due to vaporization of liquid droplets) and any user-defined sources.

Conservation of momentum in an inertial (non-accelerating) reference frame is described by the next equation [39]:

$$\frac{\partial}{\partial t} (\rho \vec{v}) + \nabla \cdot (\rho \vec{v} \vec{v}) = -\nabla p + \nabla \cdot (\bar{\tau}) + \rho \vec{g} + \vec{F} \quad (2)$$

where p is the static pressure, $\bar{\tau}$ is the stress tensor (described below), $\rho \vec{g}$ is the gravitational body force and \vec{F} represent external body forces (for example, those arising from interaction with the dispersed phase). \vec{F} also contains other model-dependent source terms such as porous-media and user-defined sources.

3.1 Geometry and meshing

Geometry and meshing are part of the preprocessing phase to resolve a computational fluid dynamics problem. The definition of the key features of our model starts with the idea of simulating a water flow through a porous zone formed by a thin layer of zeolite applied over a layer of soil. This model consists of a vertical arrangement of a packed bed like porous zone formed by the two layers, both contained in a transparent pipe with a water flow from top to bottom applied by gravity. PTC-CREO [40] was used to develop the 3D CAD model needed so CAE software may be enabled to carry on with the CFD simulation. SpaceClaim is a module within ANSYS used to prepare geometries for CFD calculations [37] and, it was used to extract the fluid domain for the meshing procedures. The module ANSYS meshing was used to carry on with the meshing procedure of the fluid domain.

3.2 Porous media model

The porous media model incorporated in ANSYS-Fluent can be used in a wide variety of single phase and multiphase problems, for example, flow through packed beds, filter papers, perforated plates, flow distributors, and others.

In this model, a cell zone is selected as the porous media where ANSYS methodology is applied by means of user inputs and the Momentum Equations for Porous Media, for further information the reader is referred to the ANSYS-Fluent manual [38].

3.3 Limitations and assumptions of the porous media model

The porous media model incorporates an empirically determined flow resistance in a region of your model defined as “porous”. In essence, the porous media model adds a momentum sink in the governing momentum Equations [38]. The model would represent a porous zone without a detailed exact model of the porosity within the materials at microscale, in other words, the porous zone will be represented

qualitatively and will be resolved with equations empirically defined to do so as explained briefly in the next paragraphs.

3.4 Momentum equations for porous media

The porous media models for single phase flows and multiphase flows use the Superficial Velocity Porous Formulation as the default. ANSYS Fluent calculates the superficial phase or mixture velocities based on the volumetric flow rate in a porous region.

Porous media are modeled by the addition of a momentum source term to the standard fluid flow equations. The source term is composed of two parts: a viscous loss term (Darcy's equation first term on the right-hand side, and an inertial loss term (Darcy's equation second term on the right-hand side), as shown next:

$$S_i = - \left(\sum_{j=1}^3 D_{ij} \mu v_j + \sum_{j=1}^3 C_{ij} \frac{1}{2} \rho |v| v_j \right) \quad (3)$$

where S_i is the source term for the i -th (x , y , or z) momentum equation, $|v|$ is the magnitude of the velocity and D and C are prescribed matrices. This momentum sink contributes to the pressure gradient in the porous cell, creating a pressure drop that is proportional to the fluid velocity (or velocity squared) in the cell which enables a viable calculation route without the need of microscale porosity details.

To recover the case of simple homogeneous porous media

$$S_i = - \left(\frac{\mu}{\alpha} v_i + C_2 \frac{1}{2} \rho |v| v_i \right) \quad (4)$$

where α is the permeability and C_2 is the inertial resistance factor, simply specify D and C as diagonal matrices with $1/\alpha$ and C_2 , respectively, on the diagonals (and zero for the other elements).

ANSYS Fluent also allows the source term to be modeled as a power law of the velocity magnitude [38]:

$$S_i = -C_0 |v|^{C_1} = -C_0 |v|^{(C_1-1)} v_i \quad (5)$$

where C_0 and C_1 are user-defined empirical coefficients.

Important

In the power-law model, the pressure drop is isotropic and the units for C_0 are SI but we will not enter any further in the mathematical model supporting this idea and will refer the reader to ANSYS manuals and proper references contained in there to develop this model in part or in whole at the reader convenience.

3.5 Darcy law and Darcy-Forchhimer

In laminar flows through porous media, the pressure drop is typically proportional to velocity and the constant can be considered zero. Ignoring convective acceleration and diffusion, the porous media model then reduces to Darcy's Law [38]:

$$\nabla p = - \frac{\mu}{\alpha} \vec{v} \quad (6)$$

Pressure drop is computed in ANSYS Fluent for each one of the three (x , y , z) coordinate directions within the porous region according to:

$$\begin{aligned}\Delta p_x &= \sum_{j=1}^3 \frac{\mu}{\alpha} v_j \Delta n_x \\ \Delta p_y &= \sum_{j=1}^3 \frac{\mu}{\alpha} v_j \Delta n_y \\ \Delta p_z &= \sum_{j=1}^3 \frac{\mu}{\alpha} v_j \Delta n_z\end{aligned}\tag{7}$$

where $1/\alpha_{ij}$ are the entries in the matrix D in Eq. (3), v_i are the velocity components in the x , y , and z directions, and Δn_x , Δn_y , and Δn_z are the thicknesses of the medium in the x , y , and z directions.

Here, the thickness of the medium (Δn_x , Δn_y , or Δn_z) is the actual thickness of the porous region in our model. Therefore, if the thicknesses used in the model differ from the actual thicknesses, adjustments may be needed in the inputs for $1/\alpha_{ij}$.

Calculations for laminar flow regime models were based in Darcy law. For calculations under turbulent flow regime Darcy-Forchhimer is the mathematical model used by ANSYS.

3.6 Processing

This work was processed using ANSYS Fluent®. The pressure–velocity coupling scheme controls the way pressure and velocity are updated when the pressure-based solver is used. The scheme can be either segregated (pressure and velocity are updated sequentially) or coupled (pressure and velocity are updated simultaneously) [38]. The scheme used in this work for pressure–velocity coupling is SIMPLE. For spatial discretization we use least squares cell based for gradient, PRESTO! for pressure and second order upwind for momentum. This set up was successful to treat single layer and double layer porous media models and convergence was reached with few to moderate number of iterations.

3.7 Postprocessing

The results module provided by ANSYS® was used to visualize code/numerical results, the data may be presented in different ways to facilitate the numerical analysis. The figures and graphs were generated from the numerical sheet produced within ANSYS-Fluent. These may include domain geometry and grid display, vector plots, line, and shaded contour plots, 2D and 3D surface plots, particle tracking, and view in perspective (translation, rotation, scaling, etc.), and few hand-made numerical computations.

4. Results and discussion

This work was developed using computational fluid dynamics (CFD) as implemented in ANSYS-Fluent. The calculation processes are explained in the next paragraphs.

4.1 Geometry and meshing

The geometries and assemblies initially were developed using CAD programs, but they can be designed either way in the geometry module within ANSYS, which

is called SpaceClaim. A CAD program enables further development and a highly detailed design, which is interesting for complex developments. For the scope of this work, SpaceClaim was used to prepare the geometry for CFD. **Figure 1** shows the geometry preparation in different steps up to the meshing generation.

Meshing procedure was carried on ANSYS meshing module, since the geometry is a simple cylinder, the discretization process was easily resolved. The meshing model was carried on systematically with a different number of elements, from a

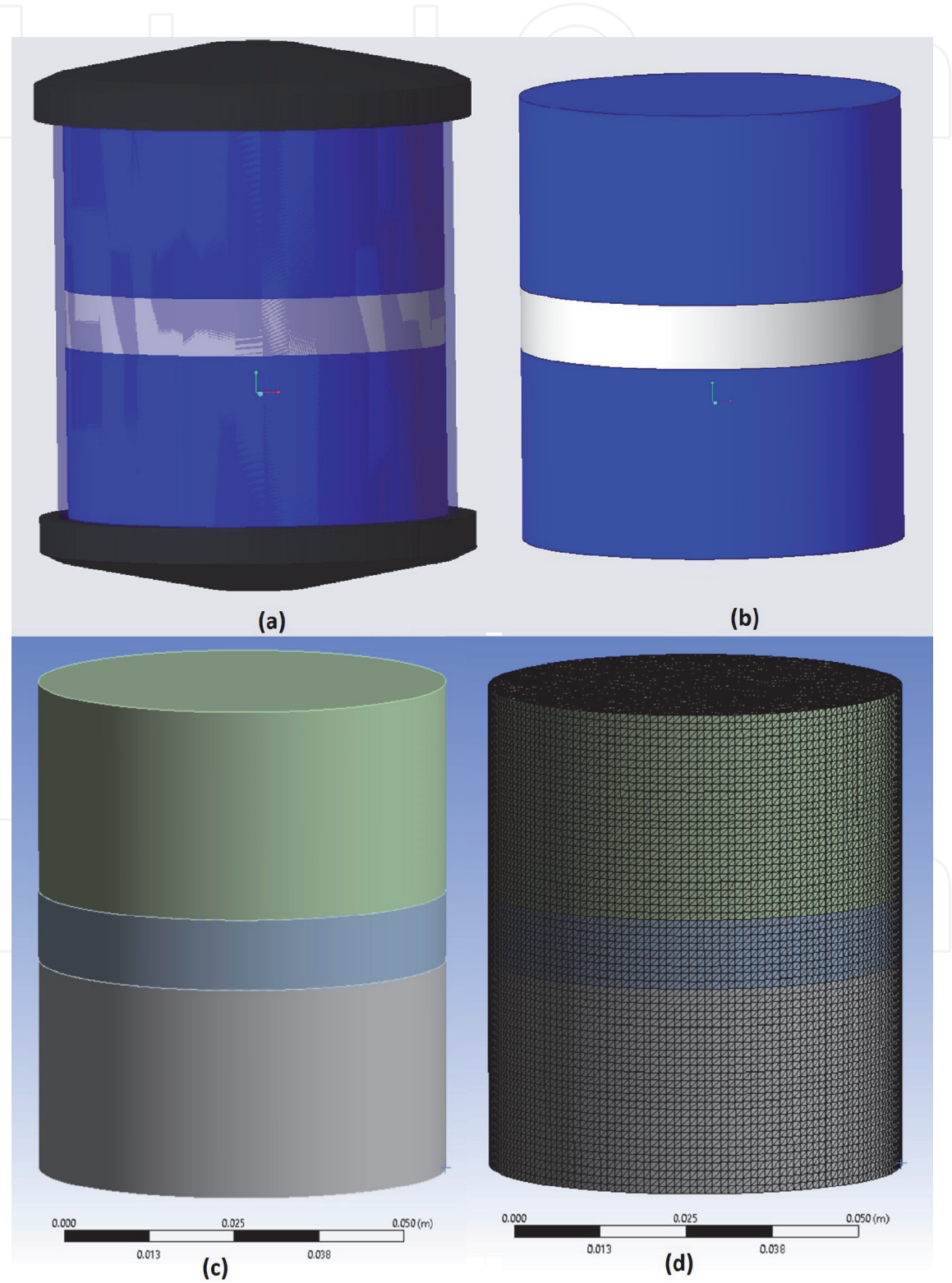


Figure 1. Geometry used to simulate a single layer of zeolite exposed to water flow from top to bottom. (a) CAD geometry for zeolite single layer interacting with water, (b) CAD geometry of fluid and porous zone without pipe and covers. (c) Fluid domain prepared in ANSYS for CFD simulation, (d) meshed fluid domain.

rough mesh to a finer mesh in search of the more efficient model. Overall, under 100 thousand elements was considered a rough mesh, up to 500 thousand elements is medium and over that number of elements is considered a fine mesh. The models used in 3D demonstrated a nice performance during the convergence trials (**Figure 2**), however, if a further simplification is found, it should be considered.

Therefore, 2D models were developed to improve efficiency in our calculations. The 2D model worked very well and improved efficiency so we decided to present the results generated with these models.

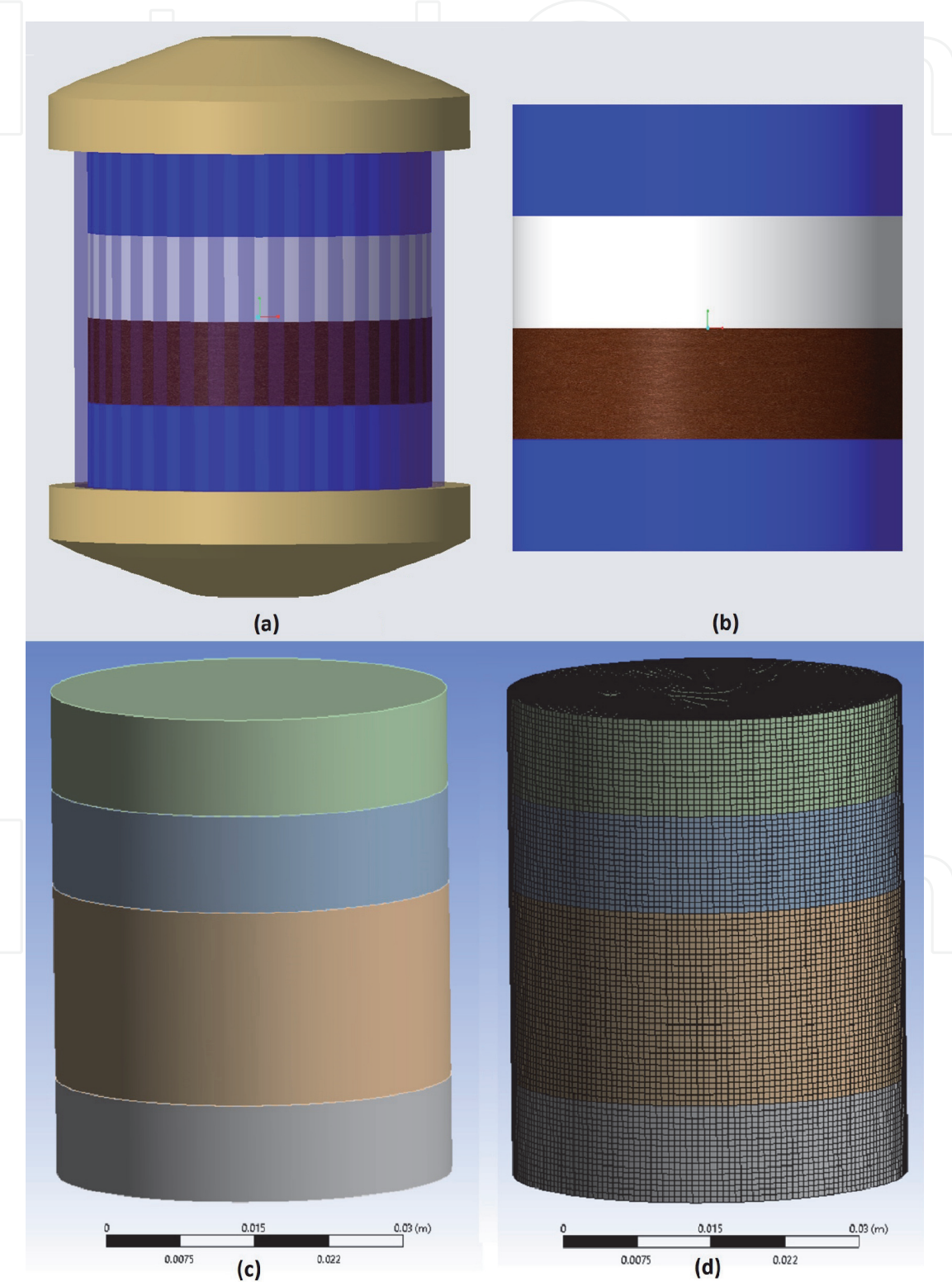


Figure 2.
Geometry used to simulate a layer of zeolite over a layer of soil exposed to water flow from top to bottom. (a) CAD geometry for zeolite-soil porous layers interacting with water, (b) CAD geometry of fluid and porous zone without pipe and covers. (c) Fluid domain prepared in ANSYS for CFD simulation, (d) meshed fluid domain.

Overall, the best results were obtained with simplified models using a 2D geometry representative of the proposed systems with single and double porous media layer, an example of 2D model geometry used is shown in **Figure 3**. The figure illustrates a slice of the interacting materials stacked from top to bottom with a first layer of water on top, followed by two layers composed with porous materials ordered in zeolite placed over soil and at the bottom more water. **Figure 3(a)** was obtained from ANSYS SpaceClaim where it may be optional to label each layer but also labels may be added in the meshing module. The geometry was simplified to a basic shape, as can be observed in **Figure 3(b)**. Thus, the model was easily

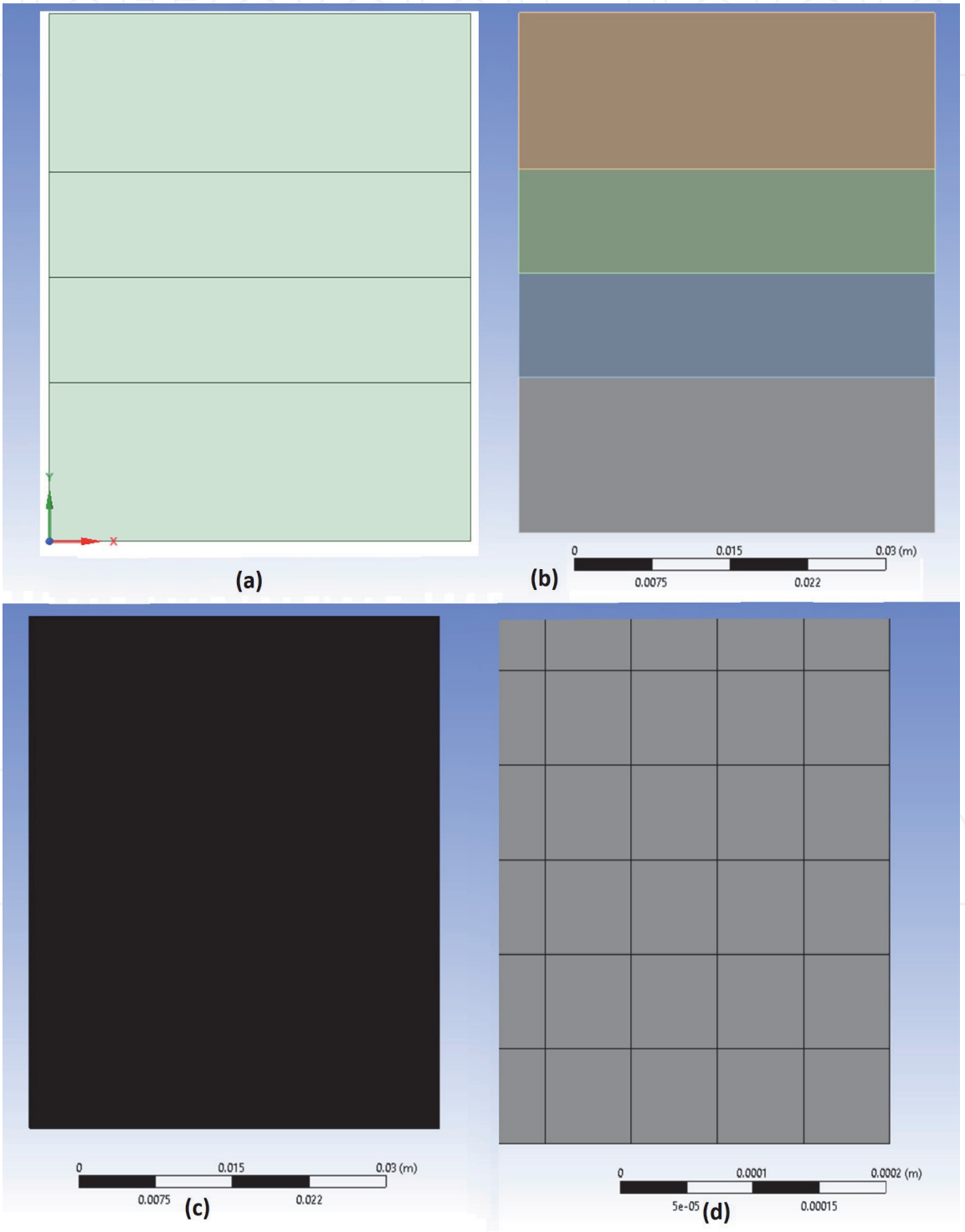


Figure 3. Simplification to a 2D model of the double layer with soil zeolite on top of soil as loaded in ANSYS for meshing procedures and mesh obtained (see scale for length dimensions under the model image).

discretized by using ANSYS meshing module with an average size element of 6.5×10^{-5} m (0.065 mm) which in total added up to 473,550 elements. The discretization results may be observed in **Figure 3(c)** and **(d)**.

4.2 Solution

Convergence trials were carried on with different geometries and resolution models. The best choice was selected based in efficiency and 2D models were selected over 3D. The geometries proposed were designed as simple models, the idea is a simple pipe containing a packed bed formed with one or two porous materials layers.

These geometries were used in calculations under laminar and turbulent flow regime set up subject to boundary conditions. Calculations with double layer and under both flow regimes are included in the following sections for a more detailed discussion of results.

4.3 Laminar flow regime

Two different set of calculations are presented in the next paragraphs, the first one is based in results obtained from laminar flow regime models. Results for pressure calculations are presented in **Figure 4**. These calculations required an input velocity with different values relatively low to obtain laminar flow through a double layer porous zone built with zeolite and soil. Velocity values used in this section are $v_1 = 0.005$ m/s, $v_2 = 0.01$ m/s, $v_3 = 0.02$ m/s, $v_4 = 0.03$ m/s, and $v_5 = 0.04$ m/s.

Pressure effects are displayed in **Figure 4**, to understand pressure-drop in a layer-by-layer contour plot that illustrates water flow moving through zeolite and soil layers modeled as porous media within ANSYS-Fluent.

The higher the input velocity, the higher pressure is required to make the flow pass through the porous media, for specific pressure values a scale in pascals is shown by the side of each simulation to help interpret the contours color in the image.

In **Figure 5** are presented contour plots of velocity to illustrate how water is applied gradually into the model. Water is applied using an input velocity with low values to keep the flow under laminar regime in y-axis negative direction (downwards). Velocity decreases as the flow advances through the pipe and porous zone represented by the two layers simulating zeolite and soil. Each velocity contour plot includes a scale with velocity values in meters per second to facilitate the interpretation of each color included in the contour plot. For a better understanding of pressure drop, a graph showing pressure drop profile was generated based in results for laminar flow regime computations as displayed in **Figure 6**. This profile is built as a scatter plot using y-axis or height in the model as the *x-coordinate* or abscissa and, pressure drop was represented in the *y-ordinate*. The scatter plot displays an overall view of the pressure drop as y-axis values change through the pipe and porous zone. To analyze further the effects on pressure drop for laminar flow regime simulations, pressure values at different locations were calculated, specifically, at the inlet and outlet for each layer of porous media zone (boundaries). Also, pressure drop for each layer was calculated by finding the difference between pressure values at layers inlet and outlet (this difference will be referred to as delta pressure values). **Table 1** contains pressure and delta pressure calculations numerical results.

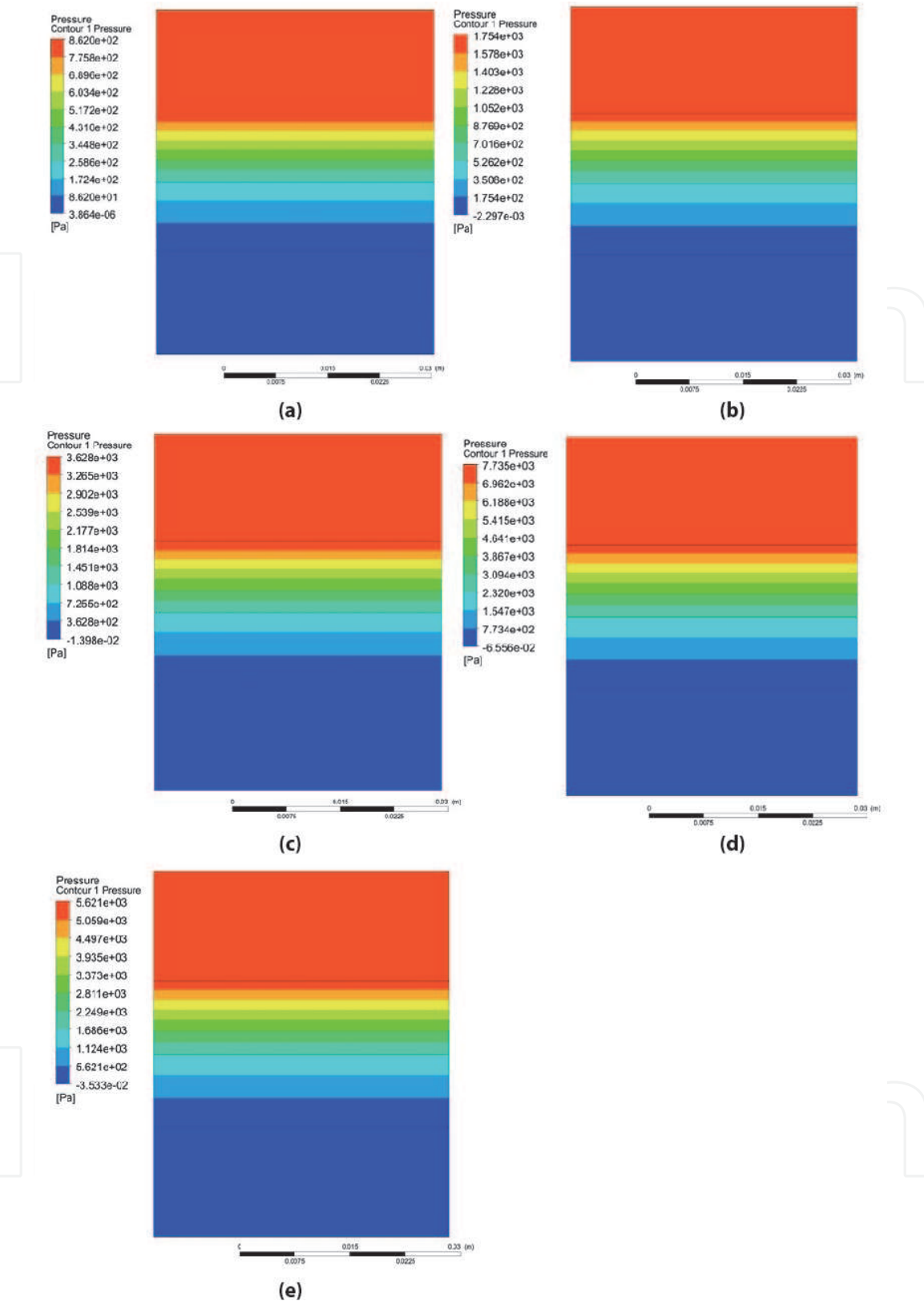


Figure 4. Contour plots corresponding to results for pressure from laminar flow regime calculations using a double layer model porous zone. (a) $v_1 = 0.005 \text{ m/s}$, (b) $v_2 = 0.01 \text{ m/s}$, (c) $v_3 = 0.02 \text{ m/s}$, (d) $v_4 = 0.03 \text{ m/s}$, (e) $v_5 = 0.04 \text{ m/s}$.

4.4 Turbulent flow regime

Results for pressure calculations obtained from turbulent flow model simulations are presented in **Figure 7**. These calculations required an input velocity with different values to obtain turbulent flow through our model with a double layer porous zone built with zeolite and soil.

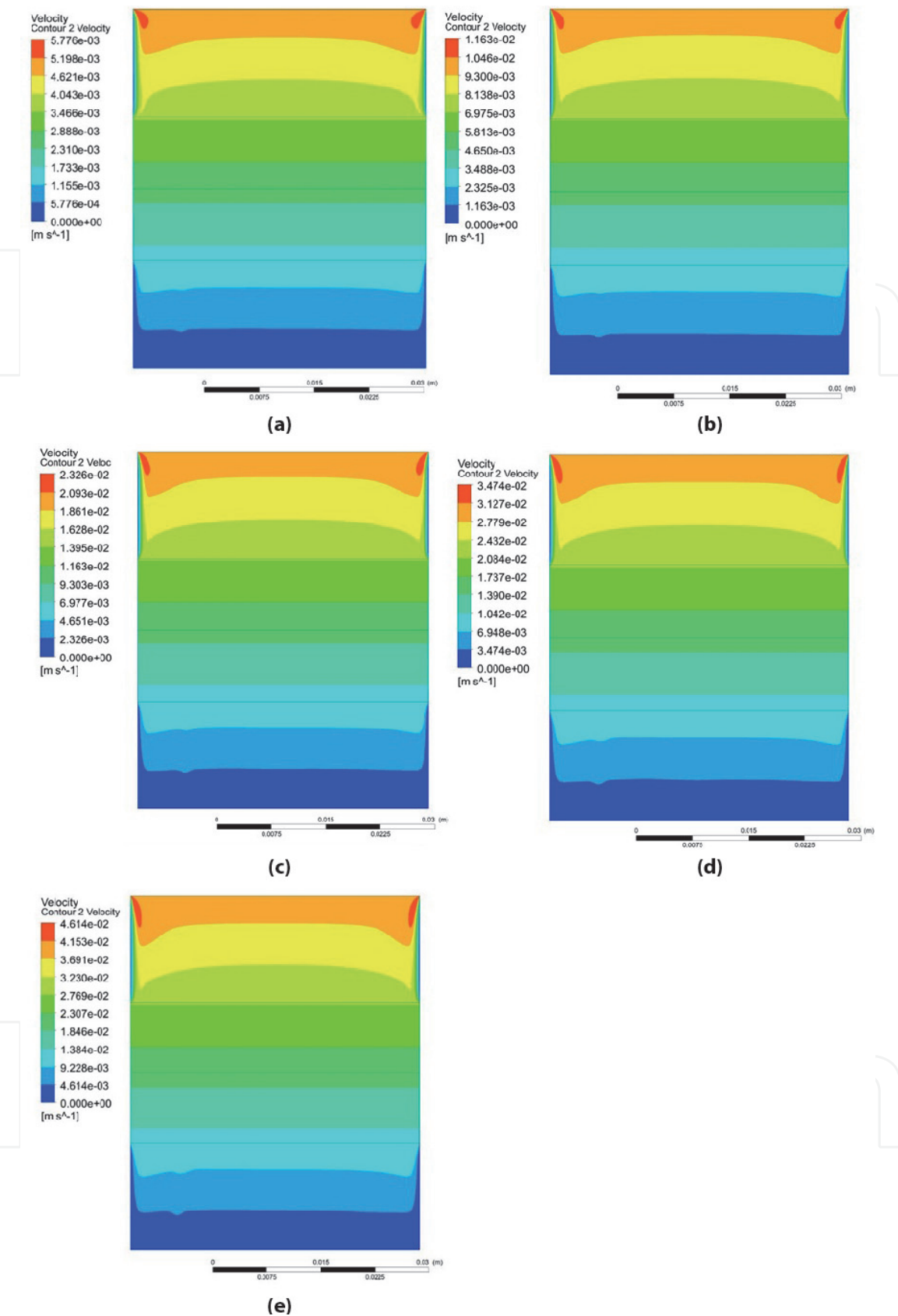


Figure 5. Contour plots corresponding to results for velocity in y-direction from laminar flow regime calculations using a double layer model porous zone. (a) $v_1 = 0.005 \text{ m/s}$, (b) $v_2 = 0.01 \text{ m/s}$. (c) $v_3 = 0.02 \text{ m/s}$, (d) $v_4 = 0.03 \text{ m/s}$, (e) $v_5 = 0.04 \text{ m/s}$.

Velocity values used in this section are $v_1 = 0.04 \text{ m/s}$, $v_2 = 0.05 \text{ m/s}$, $v_3 = 0.1 \text{ m/s}$, $v_4 = 0.2 \text{ m/s}$, $v_5 = 0.3 \text{ m/s}$, $v_6 = 0.4 \text{ m/s}$, $v_7 = 0.5 \text{ m/s}$. Pressure effects as displayed in **Figure 7** represent pressure drop for our models under turbulent flow regime in a

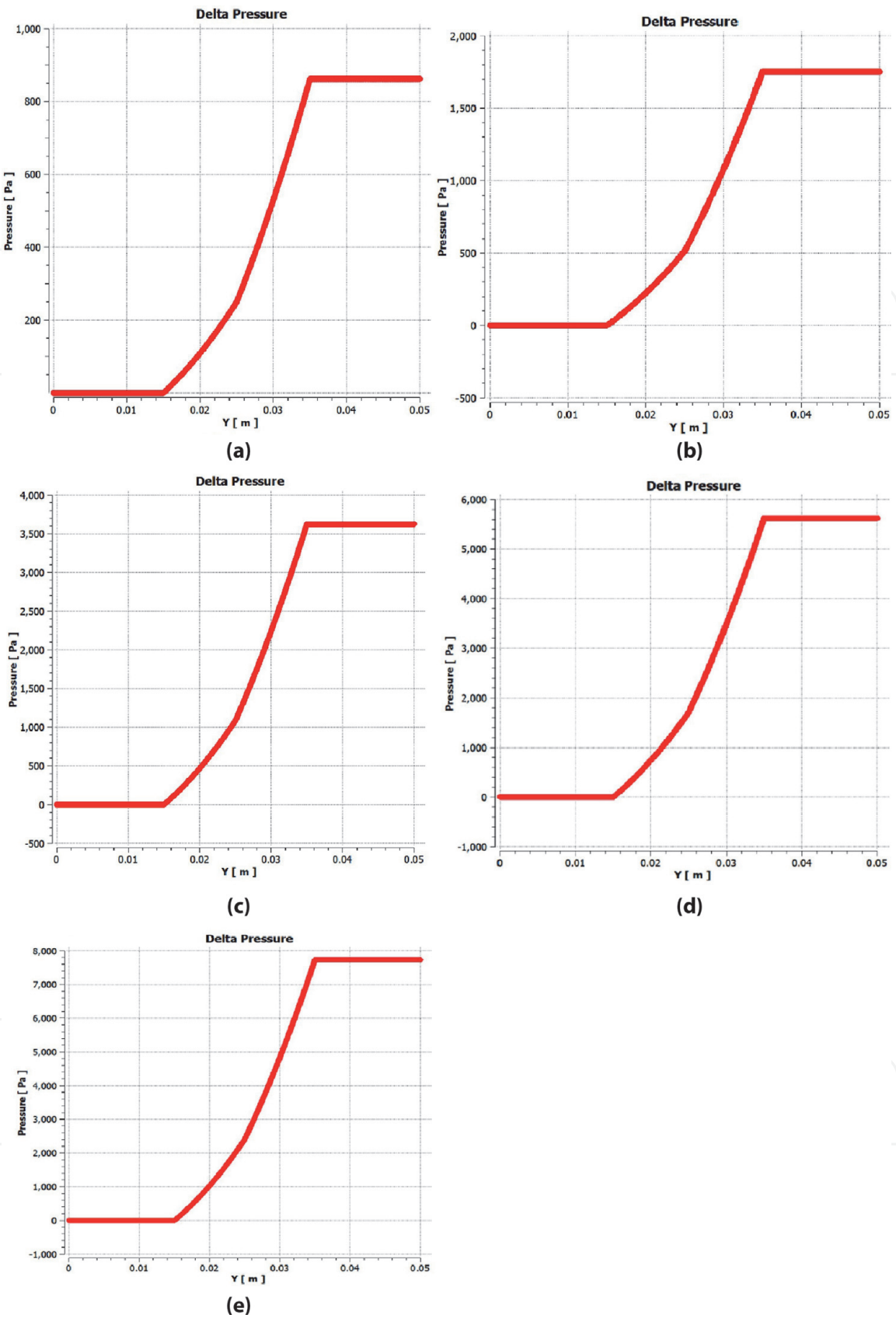


Figure 6. Graph showing pressure drop results for laminar flow regime calculations using a double layer model porous zone. (a) $v_1 = 0.005$ m/s, (b) $v_2 = 0.01$ m/s, (c) $v_3 = 0.02$ m/s, (d) $v_4 = 0.03$ m/s, (e) $v_5 = 0.04$ m/s.

layer-by-layer contour plot to illustrate water flow through zeolite and soil layers modeled as porous media within ANSYS-Fluent.

The higher the input velocity, the higher pressure is required to make the flow through the porous media, for specific pressure values a scale in pascals is shown by

v (m/s)	$P_{\text{inlet-zeol}}$ (Pa)	$P_{\text{outlet-zeol}}$ (Pa)	$P_{\text{inlet-soil}}$ (Pa)	$P_{\text{outlet-soil}}$ (Pa)	ΔP_{zeol} (Pa)	ΔP_{soil} (Pa)	ΔP_{Total} (Pa)
0.005	862	603.4	258.6	86.2	258.6	172.4	775.8
0.01	1754	701.6	526.2	175.4	1052.4	350.8	1578.6
0.02	3628	1451	1088	362.9	2177	725.1	3265.1
0.03	7735	3094	2320	773.4	4641	1546.6	6961.6
0.04	5621	2249	1686	562.1	3372	1123.9	5058.9

Table 1.
Laminar flow regime pressure-drop numerical results at the boundaries between different layers (zeolite over soil) to analyze flow through porous zone.

the side of each simulation to help interpret the contours color in the image. In comparison with laminar flow, water flow velocity and pressure present higher values.

In **Figure 8** are presented contour plots of velocity to illustrate how water flows through the porous zone. Water is applied using an input velocity with low values just enough to keep the flow as turbulent with a direction in y-axis with or without negative sign (downwards).

Velocity decreases as the flow advances through the porous zone represented by the two layers simulating zeolite and soil. Each velocity contour plot includes a scale with velocity values in meters per second to facilitate the interpretation of each color included in the contour plot.

For a better understanding of pressure drop, a graph showing pressure drop profile was generated for turbulent flow calculations as displayed in **Figure 9**. Similarly, as it was done with laminar flow, the profile is built with a scatter plot using y-axis or height in our model as the *x-coordinate* and pressure drop is represented in the *y-ordinate*. Also, to analyze further the effects on pressure drop for laminar flow regime simulations, pressure values at the boundaries for each layer of the porous media zone. Pressure drop for each layer in the turbulent model was calculated by finding the difference between pressure values at layers considering an inlet and an outlet. **Table 2** contains pressure and delta pressure numerical results.

4.5 Effects on zeolite and soil layers

Porous zone flow is simulated as a region that presents resistance to the fluid flow. When water is introduced in the system each layer representing a porous material presents a difficulty to allow flow through which can be measured with the pressure drop calculated on those areas. Due to its properties, zeolite layer presents the higher pressure drop values. Zeolite and soil material parameters to represent materials properties used within this work are based in textbook values [1, 8, 35] and can be modified as required depending on the specific properties of the materials that need to be simulated. The input velocity is also important regarding how pressure drop displays its profile and relative values, in general, the higher the input velocity value, the higher the pressure drop in the porous zone areas. Such effect occurs in laminar flow and turbulent flow. However, pressure drop may be higher in turbulent flow due to velocity input values are higher too. This model may be useful for future developments where the porous materials properties are modified or when one needs further studies related to water distribution in the system.

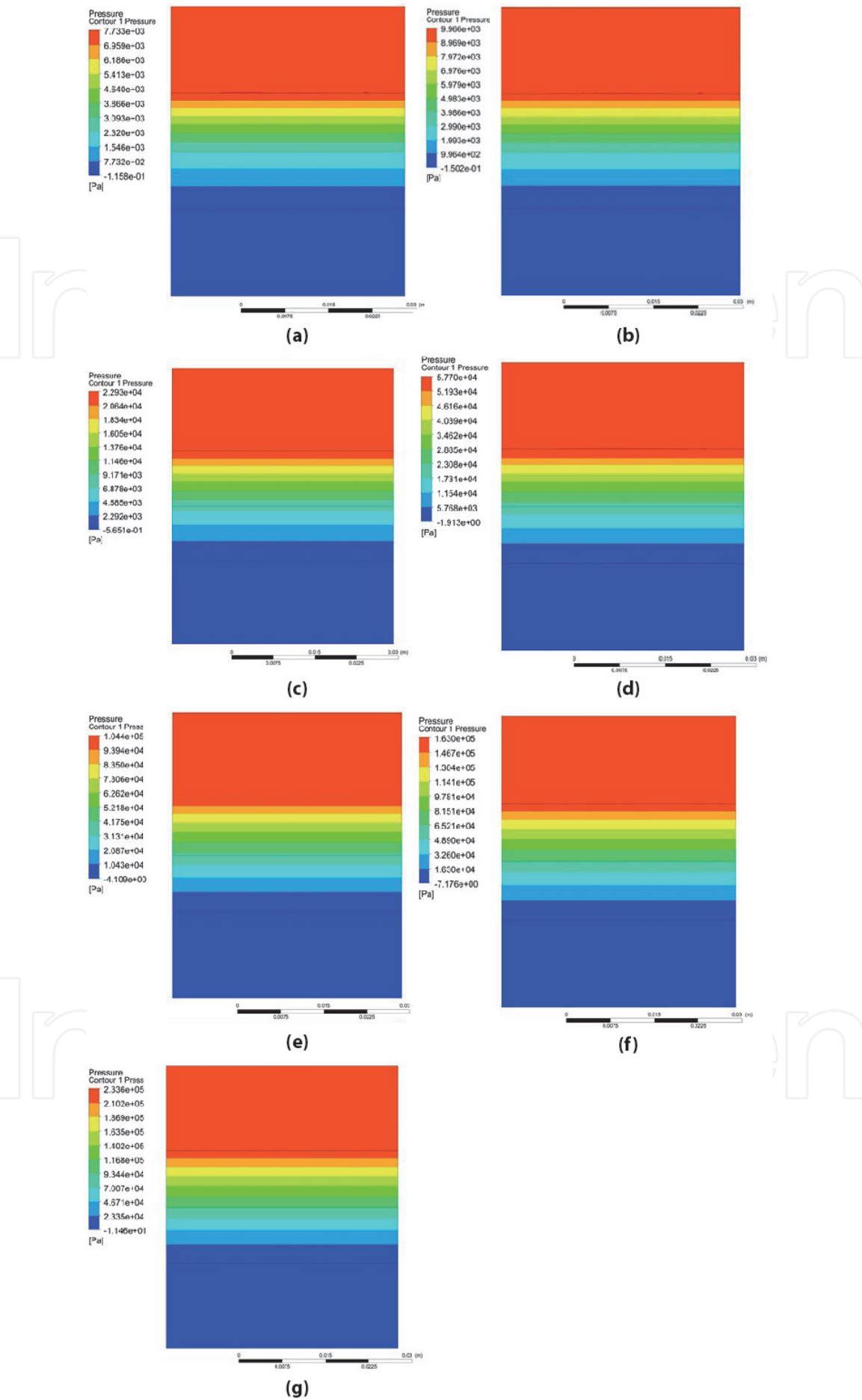


Figure 7. Contour plots for pressure obtained from turbulent flow regime numerical results corresponding to calculation with different velocity inputs using a double layer porous zone, the velocity values used were: (a) $v_1 = 0.04$ m/s, (b) $v_2 = 0.05$ m/s, (c) $v_3 = 0.1$ m/s, (d) $v_4 = 0.2$ m/s, (e) $v_5 = 0.3$ m/s, (f) $v_6 = 0.4$ m/s, (g) $v_7 = 0.5$ m/s.

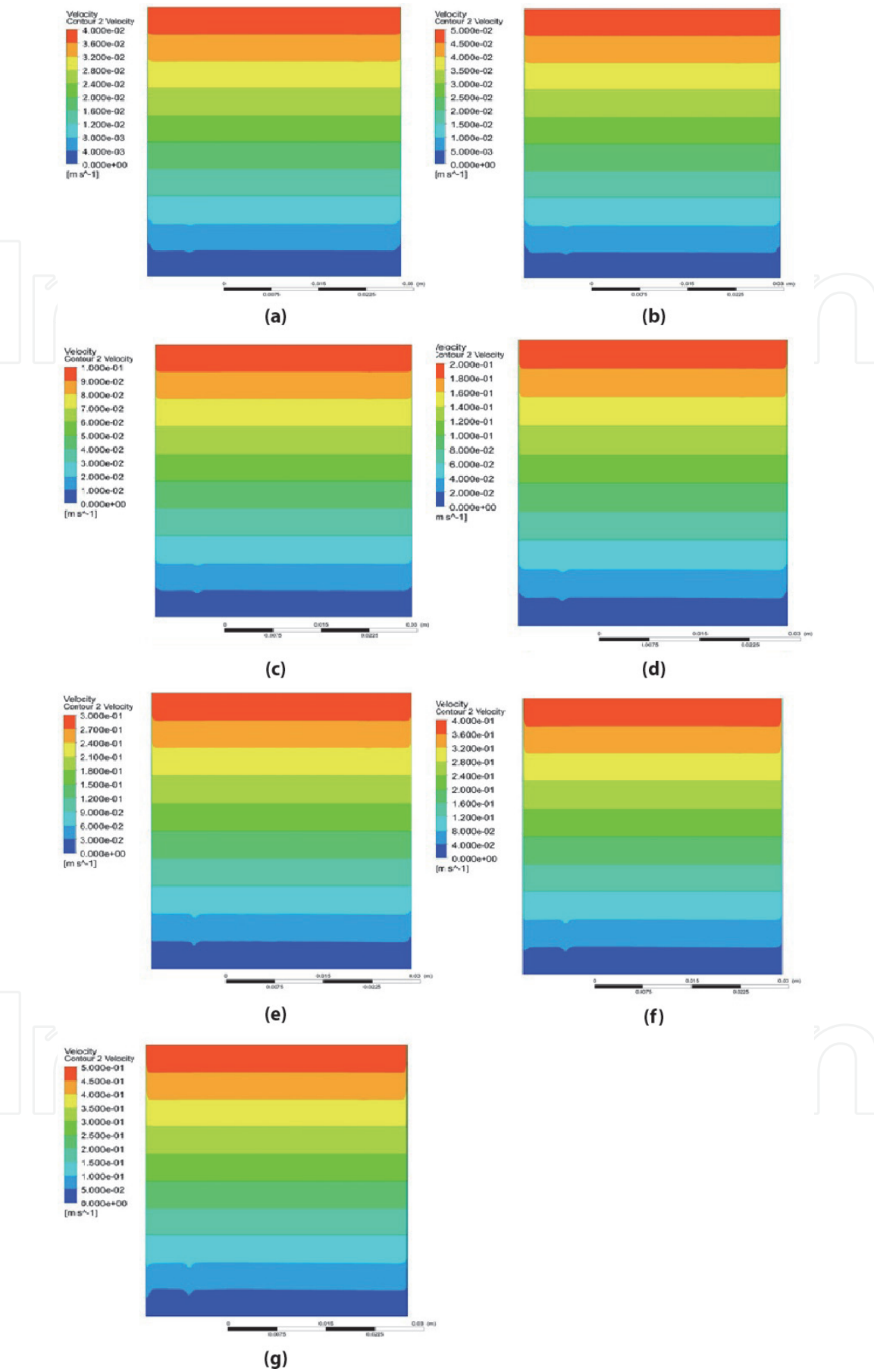


Figure 8.
Contour plots for velocity in y-axis obtained from turbulent flow regime numerical results corresponding to calculations with different velocity inputs using a double layer porous zone, the velocity values used were: (a) $v_1 = 0.04$ m/s, (b) $v_2 = 0.05$ m/s, (c) $v_3 = 0.1$ m/s, (d) $v_4 = 0.2$ m/s, (e) $v_5 = 0.3$ m/s, (f) $v_6 = 0.4$ m/s, (g) $v_7 = 0.5$ m/s.

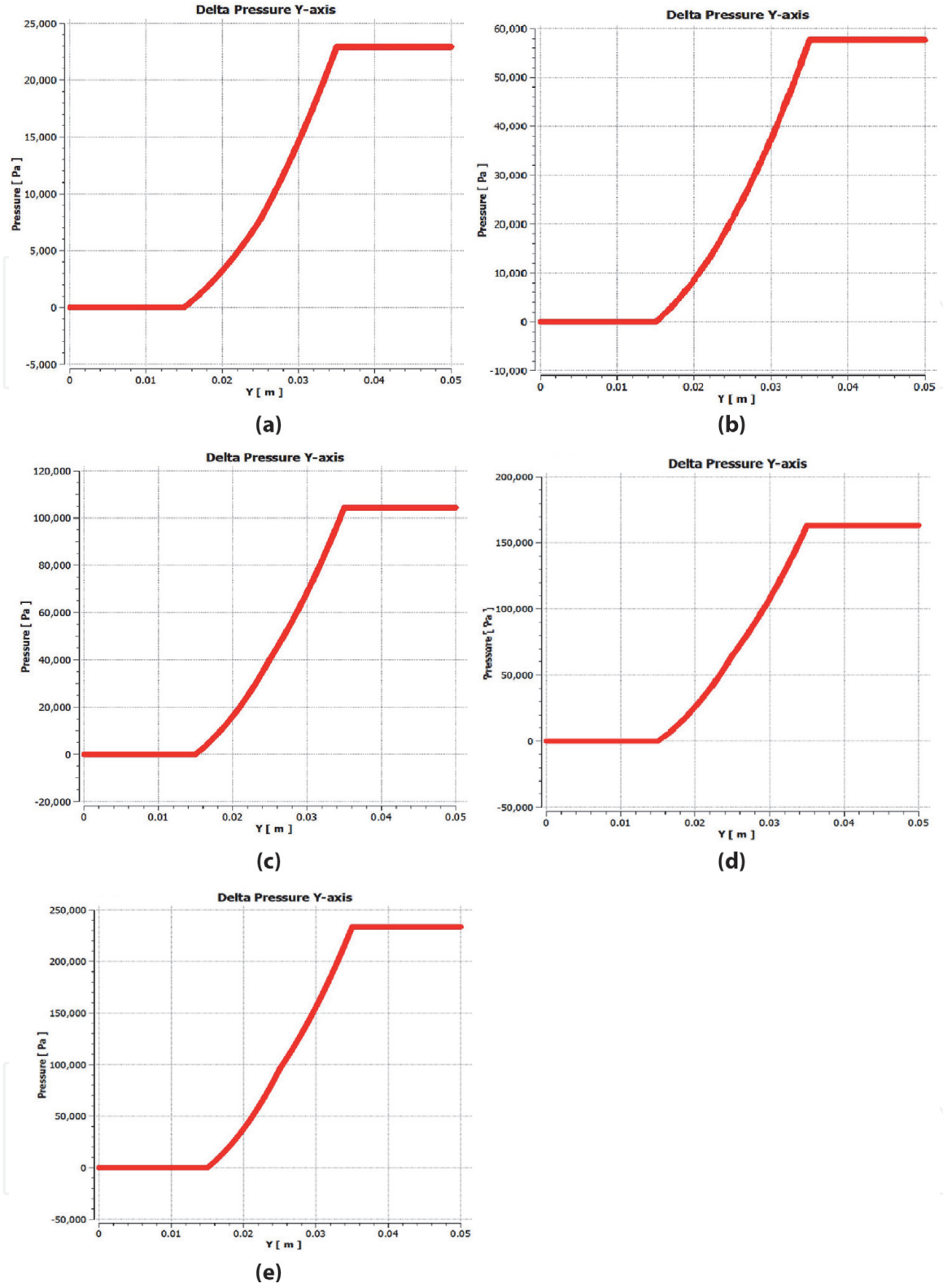


Figure 9. Graph showing pressure drop results for turbulent flow regime calculations using a double layer model porous zone. (a) $v_1 = 0.04$ m/s, (b) $v_2 = 0.05$ m/s. (c) $v_3 = 0.1$ m/s, (d) $v_4 = 0.2$ m/s, (e) $v_5 = 0.3$ m/s, (f) $v_6 = 0.4$ m/s, (g) $v_7 = 0.5$ m/s.

5. Conclusions

Computational fluid dynamics (CFD) is used as a powerful tool to analyze multi-physics problems in a wide variety of applications. To analyze porous materials ANSYS-Fluent offers an interesting scheme that enables the study of a fluid through a porous material. A bi-layer model was built to represent a layer of zeolite placed

v (m/s)	$P_{inlet-zeol}$ (Pa)	$P_{outlet-zeol}$ (Pa)	$P_{inlet-soil}$ (Pa)	$P_{outlet-soil}$ (Pa)	ΔP_{zeol} (Pa)	ΔP_{Soil} (Pa)	ΔP_{Total} (Pa)
0.04	7733	3093	2320	773.2	4640	1546.8	6959.8
0.05	9966	3986	2990	996.4	5980	1993.6	8969.6
0.1	22930	9171	6878	2292	13759	4586	20638
0.2	57700	28850	23080	5768	28850	17312	51932
0.3	104400	52180	31310	10430	52220	20880	93970
0.4	163000	81510	65210	16300	81490	48910	146700
0.5	233600	116800	93440	23350	116800	70090	210250

Table 2.
Turbulent flow regime pressure-drop calculations at the boundaries between different layers (zeolite over soil) to analyze flow through porous zone.

over a layer of soil and both interacting with a water flow. Laminar and turbulent flow regimes were analyzed successfully with the approach proposed which represents an attempt to systematically analyze different nanostructured zeolites interacting with different soil types.

Acknowledgements

This work was financed by CONACyT (Mexican Science and Technology National Council) through 2015 CONACyT SEP-CB (Basic Science-Public Education Ministry) project fund 258553/CONACyT/CB-2015-2101. Thanks go to the Scientific Computing Laboratory at FCQ-UJED for computational resources. Thanks go to the Academic Group UJED-CA-129 for valuable discussions.

Conflict of interest

The authors declare no conflict of interest.

IntechOpen

Author details

Diana Barraza-Jiménez¹, Sandra Iliana Torres-Herrera², Patricia Ponce Peña¹, Carlos Omar Ríos-Orozco³, Adolfo Padilla Mendiola¹, Elva Marcela Coria Quiñones³, Raúl Armando Olvera Corral¹, Sayda Dinorah Coria Quiñones⁴ and Manuel Alberto Flores-Hidalgo^{1*}

1 Laboratory for Scientific Computation, Faculty of Chemistry Science, Juarez University of Durango State, Durango, México


2 Faculty of Forestry Science, Juarez University of Durango State, Durango, Dgo., México

3 TecNM/Durango Institute of Technology, Durango, Dgo., Mexico

4 Cinvestav-IPN, Unidad Querétaro, Qro., Mexico

*Address all correspondence to: manuel.flores@ujed.mx

IntechOpen

© 2021 The Author(s). Licensee IntechOpen. This chapter is distributed under the terms of the Creative Commons Attribution License (<http://creativecommons.org/licenses/by/3.0>), which permits unrestricted use, distribution, and reproduction in any medium, provided the original work is properly cited. 

References

- [1] Frank A. Coutelieres, J. M. P. Q. Delgado. *Transport Processes in Porous Media*. Springer-Verlag Berlin Heidelberg 2012. DOI 10.1007/978-3-642-27910-2.
- [2] Lage, J.L., Narasimhan, A.: Porous media enhanced forced convection fundamentals and applications. In: Vafai, K. (ed.) *Handbook of Porous Media*. Marcel Dekker, New York (2000).
- [3] Ming-Hui Sun, Shao-Zhuan Huang, Li-Hua Chen, Yu Li, Xiao-Yu Yang, Zhong-Yong Yuan and Bao-Lian Su. *Chem. Soc. Rev.*, 2016,45, 3479-3563.
- [4] Arne Thomas. *Nature Communications*. (2020) 11:4985.
- [5] Zaiku Xie, Bao-Lian Su. *Front. Chem. Sci. Eng.* 2020, 14(2): 123–126.
- [6] Bao-Lian Su, Clément Sanchez, and Xiao-Yu Yang. *Hierarchically Structured Porous Materials: From Nanoscience to Catalysis, Separation, Optics, Energy, and Life Science*, 1st Edition. 2012 Wiley-VCH Verlag GmbH & Co. KGaA. 2012. Wiley-VCH Verlag GmbH & Co. KGaA.
- [7] Jonah Erlebacher and Ram Seshadri. *MRS Bulletin*. 34. 2009. 561-570.
- [8] Ruren Xu, Wenqin Pang, Jihong Yu, Qisheng Huo, Jiesheng Chen. *Chemistry of Zeolites and Related Porous Materials: Synthesis and Structure*. John Wiley & Sons (Asia). 2007. ISBN 978-0-470-82233-3.
- [9] C. Feng, K.C. Khulbe, T. Matsuura, R. Farnood, A.F. Ismail. *J. of Membrane Science and Research* 1 (2015) 49-72.
- [10] A. Maghfirah a, M.M. Ilmi a, A.T.N. Fajar b, G.T.M. Kadja. *Materials Today Chemistry* 17 (2020) 100348.
- [11] K. Zhang, M.L. Ostraat. *Catal. Today* 264 (2016) 3e15, <https://doi.org/10.1016/j.cattod.2015.08.012>.
- [12] Database of Zeolite Structures; <http://www.iza-structure.org/databases/> (Accessed November 20, 2020).
- [13] J.P. Ramirez, C.H. Christensen, K. Egeblad, C.H. Christensen, J.C. Groen. *Chem. Soc. Rev.* 37 (2008) 2530e2542, <https://doi.org/10.1039/B809030K>.
- [14] B. Smit, T.L.M. Maesen. *Nature* 451 (2008) 671e678, <https://doi.org/10.1038/nature06552>.
- [15] J. Jae, G.A. Tompsett, A.J. Foster, K. D. Hammond, S.M. Auerbach, R.F. Lobo, G.W. Huber. *J. Catal.* 279 (2011) 257e268, <https://doi.org/10.1016/j.jcat.2011.01.019>.
- [16] S. Teketel, L.F. Lundegaard, W. Skistad, S.M. Chavan, U. Olsbye, K.P. Lillerud, P. Beato, S. Svelle. *J. Catal.* 327 (2015) 22e32, <https://doi.org/10.1016/j.jcat.2015.03.013>.
- [17] M.M. Recio, J.S. Gonzalez, P.M. Torres. *Chem. Eng. J.* 303 (2016) 22e30, <https://doi.org/10.1016/j.cej.2016.05.120>.
- [18] C. Song, Y. Chu, M. Wang, H. Shi, L. Zhao, X. Guo, W. Yang, J. Shen, N. Xue, L. Peng, W. Ding. *J. Catal.* 349 (2017) 163e174, <https://doi.org/10.1016/j.jcat.2016.12.024>.
- [19] M. Koehle, Z. Zhang, K.A. Goulas, S. Caratzoulas, G.D. Vlachos, R.F. Lobo. *Appl. Catal. Gen.* 564 (2018) 90e101, <https://doi.org/10.1016/j.apcata.2018.06.005>.
- [20] X. Li, R. Xu, Q. Liu, M. Liang, J. Yang, S. Lu, G. Li, L. Lu, C. Ind. *Crop. Prod.* 141 (2019) 111759, <https://doi.org/10.1016/j.indcrop.2019.111759>.
- [21] E.T.C. Vogt, B.M. Weckhuysen. *Chem. Soc. Rev.* 44 (2020) 7342e7370, <https://doi.org/10.1039/C5CS00376H>.

- [22] Yi Li, Hongxiao Cao, and Jihong Yu. *ACS Nano* 2018, 12, 5, 4096–4104.
- [23] Bereciartua, P. J.; Cantín, Á.; Corma, A.; Jordá, J. L.; Palomino, M.; Rey, F.; Valencia, S.; Corcoran, E. W.; Kortunov, P.; Ravikovitch, P. I.; Burton, A.; Yoon, C.; Wang, Y.; Paur, C.; Guzman, J.; Bishop, A. R.; Casty, G. L. *Science* 2017, 358, 1068–1071.
- [24] Jeon, M. Y.; Kim, D.; Kumar, P.; Lee, P. S.; Rangnekar, N.; Bai, P.; Shete, M.; Elyassi, B.; Lee, H. S.; Narasimharao, K.; Basahel, S. N.; Al-Thabaiti, S.; Xu, W.; Cho, H. J.; Fetisov, E. O.; Thyagarajan, R.; DeJaco, R. F.; Fan, W.; Mkhoyan, K. A.; Siepmann, J. I.; et al. *Nature* 2017, 543, 690–694.
- [25] Jiao, F.; Li, J.; Pan, X.; Xiao, J.; Li, H.; Ma, H.; Wei, M.; Pan, Y.; Zhou, Z.; Li, M.; Miao, S.; Li, J.; Zhu, Y.; Xiao, D.; He, T.; Yang, J.; Qi, F.; Fu, Q.; Bao, X. *Science* 2016, 351, 1065–1068.
- [26] Snyder, B. E. R.; Vanelderen, P.; Bols, M. L.; Hallaert, S. D.; Böttger, L. H.; Ungur, L.; Pierloot, K.; Schoonheydt, R. A.; Sels, B. F.; Solomon, E. I. *Nature* 2016, 536, 317–321.
- [27] Shan, J.; Li, M.; Allard, L. F.; Lee, S.; Flytzani-Stephanopoulos, M. *Nature* 2017, 551, 605–608.
- [28] Primo, A.; Garcia, H. *Chem. Soc. Rev.* 2014, 43, 7548–7561.
- [29] Al-Khattaf, S.; Ali, S. A.; Aitani, A. M.; Žilková, N.; Kubička, D.; Čejka, J. *Catal. Rev.: Sci. Eng.* 2014, 56, 333–402.
- [30] Vogt, E. T. C.; Weckhuysen, B. M. *Chem. Soc. Rev.* 2015, 44, 7342–7370.
- [31] Beale, A. M.; Gao, F.; Lezcano-Gonzalez, I.; Peden, C. H. F.; Szanyi, J. *Chem. Soc. Rev.* 2015, 44, 7371–7405.
- [32] Li, Y.; Li, L.; Yu, J. *Chem.* 2017, 3, 928–949.
- [33] Li, Y.; Yu, J. *Chem. Rev.* 2014, 114, 7268–7316.
- [34] Neal S. Eash, Thomas J. Sauer, Deb O'Dell, Evah Odoi. *Soil Science Simplified 6th Edition*. 2016. John Wiley & Sons.
- [35] Gregory, P. J. *Eur. J. Soil Sci.* (2006) 57:2–12.
- [36] Garrison Sposito. *The Chemistry of Soils*. 2008. Oxford University Press, Inc.
- [37] ANSYS Fluent® Academic Research CFD, Release 18.2, 19.1.
- [38] ANSYS Fluent®. *Customization Manual*. USA: Published for licensees' users by ANSYS® INC; 2017
- [39] G. K. Batchelor. *An Introduction to Fluid Dynamics*. Cambridge Univ. Press. Cambridge, England. 1967.
- [40] PTC Creo Parametric, release 7.0. 2020. PTC Inc.